

Published in final edited form as:

Cell Host Microbe. 2012 July 19; 12(1): 47–59. doi:10.1016/j.chom.2012.05.018.

Mucosal reactive oxygen species decrease virulence by disrupting *Campylobacter jejuni* phosphotyrosine signaling

Nicolae Corcionivoschi^{2,6}, Luis A. Alvarez^{1,6}, Thomas H. Sharp^{3,4}, Monika Strengert¹, Abofu Alemka^{2,8}, Judith Mantell^{3,5}, Paul Verkade^{3,5}, Ulla G. Knaus^{1,7,*}, and Billy Bourke^{1,2,7,*}

¹Conway Institute, School of Medicine and Medical Science, University College Dublin, Dublin 4, Ireland ²National Children's Research Centre, Our Lady's Children's Hospital Crumlin, Dublin 12, Ireland ³School of Biochemistry ⁴School of Chemistry ⁵Wolfson Bioimaging Facility, University of Bristol, Bristol, England

Summary

Reactive oxygen species (ROS) play key roles in mucosal defense, yet how they are induced and the consequences for pathogens are unclear. We report that ROS generated by epithelial NADPH oxidases (Nox1/Duox2) during *Campylobacter jejuni* infection impair bacterial capsule formation and virulence by altering bacterial signal transduction. Upon *C. jejuni* invasion, ROS released from the intestinal mucosa inhibit the bacterial phosphotyrosine network that is regulated by the outer membrane tyrosine kinase Cjtk (Cj1170/OMP50). ROS-mediated Cjtk inactivation results in an overall decrease in the phosphorylation of *C. jejuni* outer membrane / periplasmic proteins including UDP-GlcNAc/Glc 4-epimerase (Gne), an enzyme required for N-glycosylation and capsule formation. Cjtk positively regulates Gne by phosphorylating an active site tyrosine, while loss of Cjtk or ROS treatment inhibits Gne activity, causing altered polysaccharide synthesis. Thus, epithelial NADPH oxidases are an early antibacterial defense system in the intestinal mucosa that modifies virulence by disrupting bacterial signaling.

Introduction

Accounting for more than 20% of all deaths under the age of 5 years, diarrhoeal disease is a major cause of mortality (Bulletin WHO 2003). *Campylobacter jejuni* is the predominant enteric bacterial pathogen in humans worldwide and *C. jejuni* infection is associated with a variety of serious sequelae including Guillain-Barre syndrome, reactive arthritis and irritable bowel syndrome (Janssen et al., 2008). Despite its importance as a pathogen little is understood of how *C. jejuni* initiates disease in the human intestine or how the intestinal mucosa responds to infection. The gastrointestinal tract and mucosal surfaces in general harbor a number of innate defense strategies to maintain epithelial integrity during challenge from pathogenic organisms (Hooper and Macpherson, 2010). The physical organization of the mucosal barrier and secretion of anti-microbial mediators constitute the first line of defense. A common microbicidal process in innate immunity is the NADPH oxidase (Nox2)-mediated release of ROS into the neutrophil phagosome for pathogen killing (Nauseef, 2007). In this sealed membrane compartment highly reactive ROS are generated

*Correspondence: ulla.knaus@ucd.ie, billy.bourke@ucd.ie Ulla G. Knaus: Tel: +353-1-7166719; Fax: +353-1-7166710 .

⁶These authors contributed equally to this work

⁷These authors contributed equally to this work

⁸Current address: Alberta Ingenuity Centre for Carbohydrate Science, University of Alberta, Edmonton, Canada

that lead to DNA and protein damage, thereby contributing to inactivation of autoinducers and protein export pathways (Rosen et al., 2009; Rothfork et al., 2004).

ROS are also generated by mucosal epithelial barrier tissues through the related oxidase complexes Nox1-p22^{phox} and Duox2-DuoxA2. While Nox1 expression is restricted to colon, Duox2 can be found in all segments of the intestinal tract (Bae et al., 2010; Rokutan et al., 2008). Pathogen-associated molecules can lead to upregulation of Nox1 or Nox1-associated regulatory proteins (Rada and Leto, 2008), implicating this oxidase in immune cell signaling. In addition, anti-bacterial properties of Duox in the intestine of *Drosophila* or zebrafish larvae have been reported (Flores et al., 2010; Ha et al., 2009). The availability of an oxygenation zone close to the epithelial surface provides a suitable milieu for production of superoxide and H₂O₂ by epithelial oxidases in the intestine (Marteyn et al., 2011). For mucosal surfaces in the lung, a role for a Duox-lactoperoxidase (LPO) system producing microbicidal hypothiocyanite has been proposed (Fischer et al., 2011; Xu et al., 2009). The relevance of this mechanism to mucosal host defense *in vivo* has not been confirmed and relies on sufficient generation of halides. However, diffusion and decomposition of ROS in the extracellular environment of the intestine will likely diminish the local concentration of ROS and therefore, if and how intestinal pathogens might be affected by ROS is not known.

Innate immune mechanisms elicited by *C. jejuni* invasion of the intestinal epithelium are essential for limiting the duration and severity of infection. *C. jejuni* appears to have evolved a repertoire of virulence mechanisms for immune avoidance. In addition to protection from environmental stress, the bacterial capsule is one of the established pathogenicity factors in *C. jejuni*. Capsule-deficient organisms show impaired colonization in chicks, decreased epithelial invasion, reduced virulence in ferrets, and are highly sensitive to complement-mediated killing (Bacon et al., 2001; Keo et al., 2011). Our earlier observations that capsule expression and virulence of *C. jejuni* are modulated by host cell factors in the extracellular milieu points to the likely involvement of an infection-dependent, diffusible signaling process between host and pathogen (Corcionivoschi et al., 2009).

Here, we examined the possibility that H₂O₂ represents the soluble host factor released from the human intestinal epithelium following infection by *C. jejuni*. Upon contact with the bacterium NADPH oxidases were redistributed to the bacterial entry site resulting in release of H₂O₂ into the extracellular environment at the mucosal surface. Continuous exposure to low concentrations of H₂O₂, as encountered by bacteria in the intestine, was sufficient to alter bacterial signal transduction, i.e. disruption of the *C. jejuni* phosphotyrosine network located in the outer membrane and periplasmic space. An unconventional *C. jejuni* bacterial tyrosine kinase (BY-kinase) was identified that controlled capsule formation by phosphorylating an epimerase involved in polysaccharide biosynthesis. Thus, epithelial NADPH oxidases function as an innate mucosal defense system by targeting bacterial phosphotyrosine signaling to modulate pathogenicity.

RESULTS

***Campylobacter* infection triggers Nox1/Duox2-mediated ROS generation**

We reported that host epithelial cells modulate *C. jejuni* virulence by an unidentified mechanism (Corcionivoschi et al., 2009). With immune defense systems in mind, we hypothesized that the release of ROS from intestinal epithelium infected by *C. jejuni* was responsible for this effect. Indeed, here we show that co-culture of *C. jejuni* 81-176 with HCT-8 intestinal epithelial cells triggered the release of H₂O₂ into the medium (Figure 1A). H₂O₂ levels rose progressively within 30 minutes following infection and stabilized after 3 hours (Figure 1B). Addition of catalase (CAT) or pretreatment of cells with the flavoenzyme inhibitor diphenylene iodonium (DPI) confirmed the presence of H₂O₂ in the medium and

the likely involvement of NADPH oxidase as a ROS-generating enzyme system (Figure 1C). *In vivo* the intestinal epithelium expresses predominantly either Nox1 (colon) or Duox2 (small bowel) (Bedard and Krause, 2007). ROS were also induced following co-culture of *C. jejuni* with cells that harbor Nox1 and Duox2, respectively (Figures 1D, E). RT-PCR experiments indicated expression of the Nox1 complex including NoxA1 and NoxO1, but not of any other NADPH oxidase isoforms in HCT-8 cells (Figure 1F). Transcriptional upregulation of the Nox1 complex or of other Nox/Duox family members was not detected, as predicted by the rapid onset of ROS generation. Supporting these observations knockdown of Nox1 attenuated H₂O₂ production by HCT-8 cells when co-cultured with *C. jejuni* (Figure 1G). Confocal images of uninfected versus *C. jejuni*-infected HCT-8 cells revealed infection-dependent redistribution of the Nox1-p22^{phox} complex to areas of lamellipodia formation and to points of entry of *C. jejuni* organisms (Figure 1H, Figures S1A-F).

We wished to confirm the *in vivo* relevance of these findings and established a polarized *ex vivo* organ culture model created from human biopsy tissues taken from normal large and small intestine at the time of routine endoscopy. Nox1 was highly expressed in colon tissue (Ct 28), while Duox2 expression in healthy, non-inflamed duodenum and colon tissues was variable (Ct 32-36, Figure S2A). Phagocyte-specific Nox2 expression was low (Ct 34-35), confirming that biopsies originated from healthy, non-inflamed tissue. Using the pIVOC methodology (Figure S2B), we observed time-dependent ROS production following *C. jejuni* challenge of the apical surface of duodenum and colon tissue (Figure 2A). This confirms that H₂O₂ is continuously released from healthy human intestinal tissue following *C. jejuni* infection. Both NADPH oxidases, Nox1 and Duox2, respond to *Campylobacter* infection in a similar manner. The activity of both oxidases was inhibited by preincubation of pIVOC organ culture with the flavoenzyme inhibitor diphenyleneiodonium (DPI). Duodenal biopsies incubated with either *C. jejuni* or with thapsigargin, which leads to Duox activation, showed maximal H₂O₂ release from these tissues, while exposure to soluble stimuli such as TNF α was less effective (Figure 2B). Confocal images of infected pIVOC tissue confirmed Duox and Nox1-p22^{phox} recruitment at sites of intimate contact of *C. jejuni* with intestinal epithelium (Figure 2C (duodenum), Figure 2D (colon)). Thus, *Campylobacter*-induced release of ROS can be detected in a human *ex vivo* model constructed to mimic conditions *in vivo* by restricting bacterial challenge to the epithelial surface of intact mucosal tissue.

Oxidase activation requires direct contact between *C. jejuni* and the host cell

In order to explore further the nature of the interaction between bacteria and eukaryotic cells that underpinned ROS production, we co-cultured *C. jejuni* and HCT-8 cells in conditions that included a filter separating *C. jejuni* from the mammalian cells. The absence of ROS production and lamellipodia formation by host cells in this setting confirmed that direct contact between *C. jejuni* and host cells is necessary for redistribution and activation of the Nox1-p22^{phox} complex, and that stimulation of cells by secreted bacterial compounds is unlikely (Figure 3A and Figure S3A). Although *C. jejuni* cannot activate human TLR5 or TLR9, and does not lead to sustained TLR4 activation in many intestinal cells, TLR2 stimulation could occur (Al-Sayeqh et al., 2010; Galkin et al., 2008; Young et al., 2007). HCT-8 cells responded to stimulation with the TLR2 ligand Malp-2 by producing ROS, but heat-inactivated *C. jejuni* failed to activate Nox1 (Figure 3B), indicating that passive host - *C. jejuni* contact is not sufficient to induce ROS generation. We confirmed the notion that active processes such as adhesion and/or invasion are required by analyzing ROS generation triggered by a *C. jejuni cadF* deletion mutant, known to have impaired ability to adhere to and invade epithelial cells (Monteville et al., 2003). Reduced invasion by absence of CadF paralleled less efficient ROS generation (Figures 3C, D). Entry of *C. jejuni* into host cells is

dependent on the actin/microtubule network (Watson and Galan, 2008; Young et al., 2007). Nocodazole or cytochalasin D treatment markedly attenuated entry of *C. jejuni* 81-176 into HCT-8 cells, membrane recruitment of Nox1 (Figure 3E, Figure S3B), and abolished ROS production (Figure 3F). Pretreatment of HCT-8 cells with the Src-family kinase inhibitor PP2 profoundly inhibited *C. jejuni* invasiveness and down-regulated ROS production (Figures 3G, H). In addition, inhibition of the GTPase Rac1 or of PI-3 kinase, both implicated in host cell entry by *C. jejuni* (Hu et al., 2006; Krause-Gruszczynska et al., 2007), caused significant reduction in ROS generation (Figure 3I). A caveat of using these inhibitors is their potential for disrupting multiple signaling pathways, as Src and Rac1 have been connected to Nox1-induced ROS generation (Gianni et al., 2010; Ueyama et al., 2006). Nevertheless, our multi-faceted approach suggests strongly that bacterial invasion serves as a trigger for mucosal ROS generation.

Hydrogen peroxide exposure impairs extracellular *C. jejuni* capsule formation and virulence

Epithelium-derived H₂O₂ present in the lumen during the course of infections will likely not irreversibly damage pathogens, but may attenuate the pathogenicity of extracellular organisms. To test if the presence of host-derived ROS alone can mediate the loss of the *C. jejuni* capsule, we exposed bacteria to H₂O₂ (Figure 4A). Capsule loss was almost complete between 50 μM and 5 mM H₂O₂, concentrations which did not alter *C. jejuni* viability or its ability to grow (Figure 4B, Figure S4A). As observed earlier with co-culture CPS depletion was detected after 6-8h of H₂O₂ exposure (Figure S4B). *C. jejuni* continuously exposed to, but separated from, direct contact with COS cells expressing Nox4 lost its capsule in a similar manner, an effect that was partially rescued by short pretreatment of cells with DPI (Figure 4C). Exogenously expressed Nox4 was used here due to its unique ability to release constitutively H₂O₂ at low rates (30-40 nmol H₂O₂ /h/mg protein) (von Lohneysen et al., 2010), while Nox1 or Duox enzymes remain dormant without stimulation. In co-culture conditions either with cells (HCT-8 cells as previously published, H661-Duox2/DuoxA2 cells Figure S4C) or with biopsies (Figure 4D) *C. jejuni* infection will trigger Nox1 or Duox2 activation, leading to ROS generation and CPS depletion. Electron microscopy of Alcian blue-stained *C. jejuni* confirmed the disappearance of the capsule polysaccharide layer upon H₂O₂ treatment, although overall morphology of *C. jejuni* was not altered (Figure 4E). For comparison, a *C. jejuni kpsM* mutant, which is deficient in high molecular weight glycan required for CPS synthesis and cannot produce a capsule, is shown. In line with CPS depletion following co-culture or genetic manipulation (Bacon et al., 2001; Corcionivoschi et al., 2009), *C. jejuni* organisms exhibited reduced adhesion (Figure 4F) and invasiveness (Figure 4G) after exposure to H₂O₂. Motility of H₂O₂ treated *C. jejuni* or *C. jejuni ΔkpsM* mutant in soft agar was attenuated (Figure 4H), presumably due to a change in bacterial surface properties following CPS depletion. In contrast, bacterial motility in liquid media was not altered (data not shown). Thus, exogenous H₂O₂ treatment of bacteria mimics the effect of intestinal co-culture on *C. jejuni* CPS production and reduces bacterial virulence.

Hydrogen peroxide shuts down phosphotyrosine signaling by a *C. jejuni* outer membrane tyrosine kinase

In eukaryotic cells ROS play a key role in modulating tyrosine phosphorylation, mainly by inhibiting protein tyrosine phosphatases. Although a much less common phenomenon in bacteria, signaling via tyrosine phosphorylation has been implicated in capsular exopolysaccharide synthesis in prokaryotes (Bechet et al., 2009b). The H₂O₂-mediated loss of CPS prompted us to analyze *C. jejuni* tyrosine phosphorylation patterns. Tyrosine phosphorylated proteins were detected in outer membrane fractions, but not in the cytosol or inner membrane fractions (Figure S5A). Co-culture with Nox1-expressing HCT-8 cells,

which is associated with capsule depletion, decreased significantly outer membrane protein (OMP) tyrosine phosphorylation in *C. jejuni* (Figure 5A). Downregulation of protein tyrosine phosphorylation was achieved within 8 hours of co-culture and was rescued by inhibition of ROS production using DPI or by decomposition of H₂O₂ using catalase (Figure 5B). A similar loss of tyrosine phosphorylation was observed in *C. jejuni* co-cultured with duodenal or colon biopsies, or with Duox2-expressing cells (Figure 5C and Figure S5B). Furthermore, exposure of bacteria to exogenous H₂O₂ (Figure 5D and Figure S5C) or to H₂O₂ produced by Cos-Nox4 cells (Figure 5E), both of which alter CPS (see Figures 4A-D), caused the disappearance of all but one tyrosine phosphorylated bands. Tryptic digest of OMPs followed by 2-D gel electrophoresis and anti-phosphotyrosine blotting revealed several tyrosine phosphorylated spots (Figure 5F I), which were lost in OMPs derived from *C. jejuni* co-cultured with cells (Figure 5F II). Thus, exposure of *C. jejuni* to H₂O₂, regardless of whether derived from epithelial cells or administered exogenously, results in greatly reduced tyrosine phosphorylation of bacterial OMPs. This finding appears to exclude ROS-mediated inhibition of a bacterial tyrosine phosphatase as mechanism causing the drop in phosphotyrosine content.

Bacterial tyrosine kinases (BY-kinases) constitute a family of recently discovered enzymes that control key regulatory prokaryotic networks (Cuthbertson et al., 2009; Lee and Jia, 2009). Previous analysis of the *C. jejuni* genome failed to identify a putative BY-kinase (Voisin et al., 2007). Using a bioinformatics approach based on homology to particular sequence motifs, we identified Cj1170c, an outer membrane protein, previously designated OMP50 (Bolla et al., 2000), as candidate BY-kinase. Based on its molecular weight we hypothesized that autophosphorylated OMP50 was represented by the remaining, tyrosine phosphorylated band at 50kDa in H₂O₂-treated or co-cultured OMP fractions. MS-MS analysis of the remaining tyrosine phosphorylated spot (Figure 5F II, indicated by arrows) followed by data base search revealed multiple OMP50-derived sequences. An antibody raised to OMP50 protein recognized a band at 50 kDa in the OMP fraction (Figure 5G) and the indicated spot in 2-D separation gels (Figure 5F III). The identity of OMP50 as the predominant tyrosine phosphorylated protein remaining in H₂O₂- or cell-exposed *C. jejuni* extracts was confirmed by analyzing a *C. jejuni* $\Delta omp50$ site-specific insertional mutant. The *C. jejuni* $\Delta omp50$ strain showed no apparent signs of major morphological changes or of growth inhibition. In OMP fractions prepared from this mutant, the band at 50kDa could not be detected by anti-OMP50 or anti-phosphotyrosine blotting (Figures 5F IV, 5G). In fact, deletion of OMP50 abolished tyrosine phosphorylation in general, indicating that this protein constitutes most likely the only BY-kinase in *C. jejuni* (Figure 5G). Next, we investigated if OMP50-deficiency would recapitulate the *C. jejuni* phenotypes observed after exposure to ROS. CPS depletion and the absence of the capsule structure indicated that OMP50 is required for polysaccharide biosynthesis or export (Figures 5H, I). Furthermore, OMP50 deficiency substantially reduced motility and invasiveness of the bacterium, coupled with significantly decreased Nox1-dependent ROS generation (Figures 5J-L), indicating that OMP50 is a major virulence factor of *C. jejuni*. To alleviate concerns regarding phase variation, we reconstituted *omp50* in the *C. jejuni* $\Delta omp50$ mutant, which reversed the motility and invasion phenotype to wildtype *C. jejuni* (Figures S5D-E). The motility phenotype could be linked to polysaccharide depletion, or might be result of the overall elimination of phosphotyrosine signaling by OMP50 deletion.

The BY-kinase OMP50 contains an essential regulatory tyrosine residue

Sequence and structural alignment of OMP50 with other known BY-kinases indicates that OMP50 represents a non-canonical prototype in this family. OMP50 is a genuine OMP, possibly forming a monomeric pore (Bolla et al., 2000), instead of following the typical BY-kinase topology in gram-negative bacteria that is characterized by two inner membrane

spanning α -helices and a cytosolic catalytic domain. The putative kinase domain in the C-terminus of OMP50 contains Walker A and Walker A' motifs, but lacks the consensus Walker B sequence (hhhhD) (Figure 6A and Figure S6). Important elements of the autoactivation switch seem to be conserved such as the combination of a putative internal regulatory tyrosine residue (Y338 OMP50, Y574 Etk) and the interacting arginine residue (R377 OMP50, R614 Etk) (Lee et al., 2008). A potential tyrosine (Y) cluster is also present, although the number and spacing of tyrosine residues is less distinctive. Minimal differences in OMP50 sequences derived from *C. jejuni* or *C. lari* exist, none of which would affect the conserved kinase motifs.

Bacterial *in vivo* tyrosine phosphorylation was examined by comparing tyrosine phosphorylation patterns of OMP fractions derived from *C. jejuni* wildtype, *C. jejuni* $\Delta omp50$ mutant and a *C. jejuni* $\Delta omp50$ strain complemented with OMP50. Deletion of OMP50 was accompanied by loss of tyrosine phosphorylation, which was recovered by OMP50 reintroduction (Figure 6B). In some, but not in all BY-kinases a regulatory tyrosine is critically involved in kinase activity (Bechet et al., 2009a). Mutation of this tyrosine to phenylalanine leads to diminished BY-kinase activity. A similar mutation in OMP50 (OMP50 Y338F) abolished *in vivo* kinase activity of OMP50 when introduced in the $\Delta omp50$ mutant background. In line with earlier observations, complementation with OMP50 Y338F reduced CPS significantly without altering OMP50 or general protein expression (Figure 6B). An OMP50 triple tyrosine mutant in the Y cluster (OMP50 Y422/425/430F) was similarly introduced into the $\Delta omp50$ strain, but did not cause any discernible phenotype, suggesting that in contrast to other BY-kinases, phosphorylation of three of the four tyrosine residues in the Y cluster is not essential for OMP50 activity towards substrates (Figure 6B). As these results indicate that OMP50 represents not only an outer membrane protein but also a BY-kinase, we propose renaming the protein Cjtk (*C. jejuni* tyrosine kinase).

***In vitro* phosphorylation of OMPs by Cjtk is ROS sensitive**

To confirm tyrosine kinase activity of Cjtk *in vitro*, we purified Cjtk from micelles prepared from *C. jejuni* wildtype OMP fractions (Figures S7A, S7B) and subjected OMP fractions derived from the $\Delta omp50$ (*cjtk*) mutant, which lack Cjtk and overall tyrosine phosphorylation, to kinase assays. The purified Cjtk was constitutively active and phosphorylated several OMP proteins on tyrosine (Figure 6C, upper panel). We then asked if addition of H₂O₂ would disrupt *in vitro* phosphorylation of OMP proteins. While autophosphorylation of Cjtk persisted, as observed earlier (Figure 5), tyrosine phosphorylation of Cjtk substrates in the Cjtk-deficient OMP fraction was substantially reduced (Figure 6C, lower panel). Thus, *in vitro* and *in vivo* tyrosine phosphorylation of proteins contained in the OMP fraction is disrupted by oxidation.

Cjtk modulates UDP-GlcNAc/Glc 4-epimerase (Gne) activity by active site tyrosine phosphorylation

How BY-kinases may regulate bacterial signaling networks becomes more apparent when the limited number of previously identified bacterial substrates is considered. One of the targets is UDP-glucose dehydrogenase (*ugd*), an enzyme involved in polysaccharide and colonic acid biosynthesis and export (Lacour et al., 2008). Tyrosine phosphorylation of bacterial proteins can lead to activation (*Ugd*, *Cap50*) or inactivation (phage integrases), or can affect general house-keeping functions such as DNA replication or heat-shock response (Bechet et al., 2009b). Loss of CPS in the *C. jejuni* $\Delta omp50$ strain pointed to modification of at least one enzyme involved in polysaccharide biosynthesis. We extracted and sequenced the five tyrosine phosphorylated spots present after 2-D separation of OMPs (see Figures 5F I, 7A). One of the proteins was identified as Cj1131c, a bifunctional UDP-GlcNAc/Glc 4-

epimerase (GalE, renamed Gne) (Bernatchez et al., 2005). The extracted tyrosine phosphorylated protein migrated at the expected molecular weight of 36 kDa (Figure 7B) and was absent when OMPs isolated from a *C. jejuni* $\Delta galE$ (*gne*) mutant were probed with anti-phosphotyrosine antibody after 2-D gel electrophoresis (Figure 7C).

Enzymes involved in carbohydrate biosynthesis are commonly expressed in the bacterial cytosol and are thought to be phosphorylated by the cytosolic kinase domain of inner membrane-associated BY-kinases. As Gne constitutes a phosphorylation target of the outer membrane kinase Cjtk, the localization of Gne in *C. jejuni* was explored. In the absence of a readily available anti-Gne antibody, we expressed histidine-tagged Gne in wildtype *C. jejuni* and probed *C. jejuni* fractions by immunoblotting with anti-histidine antibodies. Gne was present in all three fractions, although the majority of the enzyme was in membrane-associated fractions. Tyrosine-phosphorylated Gne was only present in the OMP fraction, which was expected due to the localization of Cjtk and the absence of tyrosine phosphorylation in cytosol and IMP fractions (Figure 7D and Figure S5A). Fractionations were validated by using an antibody recognizing the cytosolic ferric uptake regulator Fur and the outer membrane protein CadF.

To ascertain that Gne constitutes a genuine substrate of Cjtk, His-Gne was expressed in *E. coli*, affinity purified (Figure S7C) and subjected to kinase assays. Gne was efficiently phosphorylated by Cjtk *in vitro*, confirming Gne as Cjtk substrate (Figure 7E). Kinase assays in the presence of H₂O₂ revealed that Cjtk activity is not directly affected by H₂O₂ *in vitro* (Figure S7D). Thus, the OMP fraction contains either yet unidentified factors that permit generation of ROS with higher oxidation efficiency than H₂O₂ or provides endogenous Cjtk substrates in a structural context that is ROS sensitive. Bacterial *in vivo* phosphorylation of Gne was tested by introduction of His-Gne into *C. jejuni* wildtype and $\Delta omp50$ mutant, followed by OMP isolation and affinity purification of His-Gne. His-Gne was detected in both *C. jejuni* strains, but was only tyrosine phosphorylated in wildtype *C. jejuni* (Figure 7F). *In vitro* exposure of phosphorylated His-Gne to H₂O₂ did not remove phosphotyrosine content, indicating the structural integrity of the protein (Figure S7E). As previously described (Bernatchez et al., 2005) the $\Delta galE$ (*gne*) mutant showed pronounced loss of CPS and distinct changes in the N-glycan and lipooligosaccharide profiles (Figure 7G). The N-glycan patterns of *C. jejuni* exposed to H₂O₂ or of Cjtk-deficient ($\Delta omp50$) *C. jejuni* were similar, but revealed apparent differences when compared to the *C. jejuni* wildtype strain and the $\Delta galE$ (*gne*) strain. These results suggest that ROS exposure phenocopies the influence of Cjtk on endogenous substrates, while complete Gne deficiency leads to more pronounced changes in carbohydrate biosynthesis.

Our observations suggest that Cjtk kinase activity plays a positive regulatory role in Gne's epimerase activity. A predicted structural model of the active site of Gne places a tyrosine residue (Gne Y146) at a prominent position in the saccharide binding pocket (Bernatchez et al., 2005). This tyrosine residue is conserved throughout bacterial UDP-GlcNAc and UDP-Glc 4-epimerases. Conservative mutation of Y146 to F146 in His-Gne and expression of the wildtype or mutant enzyme in a Gne-deficient *C. jejuni* strain (*C. jejuni* 81-176 $\Delta galE$ (*gne*)) revealed that mutation of Y146 abolishes tyrosine phosphorylation of Gne (Figure 7H). Gne Y146 was also verified as Cjtk phosphorylation site *in vitro* (Figure S7F). *C. jejuni* Δgne Y146 displayed reduced CPS similar to the deletion of complete *gne* (Figure S7G). The N-glycan pattern of *C. jejuni* Δgne reconstituted with *gne* Y146F was similar to the pattern observed when analyzing the *C. jejuni* $\Delta omp50$ (*cjtk*) mutant or N-glycan patterns of *C. jejuni* exposed to host cell co-culture (Figure 7I and Figure S7H). The pattern of N-glycans changed more severely when Gne was deleted, suggesting that loss of Gne tyrosine phosphorylation by exposure to ROS or by absence of Cjtk acts as a modifier of epimerase activity. Taken together these data provide evidence for the mechanism triggering ROS-

dependent downregulation of *C. jejuni* capsular polysaccharide. In the presence of ROS, Cjtk-mediated tyrosine phosphorylation of the Gne active site (and likely those of other substrates) is defective, thereby disrupting epimerase activity necessary for efficient carbohydrate production.

DISCUSSION

We describe here a previously unappreciated role for mucosal ROS in antibacterial defense. ROS released from the intestinal epithelium in the course of *C. jejuni* infection attenuate the pathogenicity of extracellular bacteria by disrupting tyrosine phosphorylation-mediated bacterial capsule production. *C. jejuni* phosphotyrosine signaling is regulated by Cjtk, a unique member of the expanding BY-kinase family, which modifies several periplasmic and/or outer membrane proteins including an epimerase required for polysaccharide synthesis.

Given the expected rapid dispersion of ROS in an extracellular environment, the mechanism by which ROS impart host defense and exert bacterial control must differ from that of innate immune cells. Moreover, *C. jejuni* can mount a transcriptional response upon ROS exposure via the oxidative stress regulator PerR. This leads to de-repression of target genes including KatA (catalase) and AhpC (alkylhydroperoxidase), which will assist in detoxifying H₂O₂ (Palyada et al., 2009). An attractive strategy that permits mucosal ROS to achieve bacterial control by a non-microbicidal mechanism is the interference with virulence factors, thus weakening pathogenicity. A decrease in invasion of epithelial cells after exposure of *Salmonella* to H₂O₂ was described as a repellent effect of unspecified nature (Botteaux et al., 2009). As we show here, in *C. jejuni* infection this host-protective effect is afforded by disabling regulatory control of the bacterial phosphotyrosine network. Details of the mechanism for redox-mediated inactivation of *C. jejuni* phosphotyrosine signaling will require more in-depth studies, as not only Cjtk, but also its endogenous substrates and interacting protein complexes might be affected. Regulation of a bacterial enzyme by a combination of redox- and phosphorylation-dependent mechanisms has been described recently (Gruszczyk et al., 2011). An additional caveat of translating complex events triggered by exposure of bacteria to ROS to the minimalist *in vitro* phosphorylation approach using purified proteins is the loss of overall context regarding *in vivo* modifications of proteins and of the oxidant itself. Exposure of *C. jejuni* to H₂O₂ may induce the release of ferrous iron from iron-containing proteins, which will promote generation of short-lived ROS with highly increased oxidative capacity such as hydroxyl radicals (Palyada et al., 2009). The *in vivo* setting was successfully mimicked *in vitro* when utilizing purified Cjtk and the complete OMP fraction, but not when using recombinant Gne purified from *E. coli*.

We speculate that extracellular ROS could affect other invasive bacteria in a similar fashion. However, the manner in which BY-kinase networks are altered by oxidants will likely differ among bacteria, depending on the structure and location of the BY-kinase. The current model for regulating the activity of inner membrane localized BY-kinases is based on a cyclic phosphorylation-dephosphorylation process by engaging specific cytosolic low molecular weight protein tyrosine phosphatases (LMW-PTP) (ie Wzc/Wzb or Etk/Etp). Although a single LMW-PTP (Cj1258) has been identified in *C. jejuni* (Tolkatchev et al., 2006), the redox-sensitive decrease in tyrosine phosphorylation and the outer membrane location of the identified kinase Cjtk (OMP50) suggests a distinct mechanism for *Campylobacter* BY-kinase regulation. The *C. jejuni* LMW-PTP displays high overall homology to mammalian LMW-PTPs and is likely a target of oxidative inactivation, which would lead to increased phosphotyrosine content in the OMP fraction of ROS-exposed *C. jejuni* rather than to the decrease that we observe. In addition, as Cjtk-mediated

phosphorylation appears to exclude cytoplasmic proteins, the identity or localization of tyrosine phosphorylated substrates in *C. jejuni* and of the available ATP source will likely differ from other organisms. The epimerase Gne, the here identified Cjtk substrate, partitions into several bacterial compartments. It is possible that each Gne subpopulation fulfills different tasks, and certain steps require tyrosine phosphorylation.

Phosphotyrosine signaling has been linked with capsule expression in several prokaryotes (Cuthbertson et al., 2009; Grangeasse et al., 2010). Similarly, phosphoproteomic studies of *Klebsiella pneumoniae* revealed a tight connection between tyrosine phosphorylation, exopolysaccharide biosynthesis and pathogenicity of the bacterium (Lin et al., 2009). While unencapsulated/capsule-depleted pathogenic bacteria sometimes show enhanced adherence and invasion, capsule loss is predominantly associated with attenuated virulence in colonization and sepsis models of infection. Thus, ROS-induced inhibition of BY-kinase-mediated CPS expression could function as a generalized mucosal defense against encapsulated bacteria. By shutting down BY-kinase activity, a network hub, one can predict disruption of several nodes and wide-ranging effects on many bacterial species. Considering the multifunctional nature of many bacterial nodes, altering the activity or location of just one bacterial protein may impinge on several virulence determinants. A case in point is the here identified Cjtk target Gne, a UDP-GlcNAc/Glc 4-epimerase, which is required for the synthesis of three major bacterial cell surface carbohydrate structures (CPS, LOS, Pgl heptasaccharide). The pleiotropic effect on key bacterial functions by interference with BY-kinase signaling underlines their potential as promising targets for antimicrobial therapy.

The concept that ROS act as a virulence modifier in the mucosa rather than as microbicidal agent opens up new avenues of research. As much as epithelium-derived H₂O₂ is beneficial for the host during *Campylobacter* infection and likely in other bacterial infections of mucosal surfaces, it can be easily envisioned that this host response can be subverted by some pathogens to their advantage (Winter et al., 2010). In addition, although the commensal intestinal microbiota is confined to the outer loose mucus layer and thus cannot trigger mucosal ROS generation *in vivo*, changes in mucin expression in injury, inflammatory disease or cancer may provide access to the epithelium. In these circumstances, the microbiota itself may stimulate H₂O₂ release (Swanson et al., 2011), raising the possibility that microbiota-induced changes in redox balance in the lumen could modulate the pathogenicity of intestinal pathogens, or could result in aberrant microbiota. In this context, analysis of the reciprocal effects of the commensal flora and *Campylobacter* would be informative. A more complete understanding of the inter-relationships between infecting organism, resident microbiota and host mucosal Nox/Duox activation will await the development of more tractable animal models mimicking human *Campylobacter* infection.

EXPERIMENTAL PROCEDURES

Co-culture of *C. jejuni* 81-176 and *C. jejuni* mutants with cells

Agar grown bacteria were resuspended in RPMI 1640 media and cells at 60-70% confluence were incubated with 1ml of bacterial suspension (OD₆₀₀=0.4; 10⁷ bacteria). Bacteria and cells were co-cultured at 37°C using microaerobic conditions (5% O₂, 5% CO₂ and 90% N₂) for various time periods. Non-adherent bacteria were removed by centrifugation (3300g, for 5 min), and were used for isolation of CPS and the outer membrane fractions. Viable counts were performed for inocula to ensure that comparable numbers of live bacteria were present for each bacterial strain.

Polarized *In Vitro* Organ Culture (pIVOC)

pIVOC was performed using biopsy material obtained from children during routine endoscopy undertaken for clinical purposes. Between 3 and 5 biopsies were taken from normal appearing mucosa in either the third part of the duodenum or in the colon. Fully informed consent was obtained from parents and, where appropriate, children. Ethical permission was provided for this study from the Ethics Committee of Our Ladys Children Hospital Crumlin, Ireland. The pIVOC was adapted to monitor stimulated H₂O₂ production and confocal microscopy of *C. jejuni* infected mucosal epithelium. Details are described in the online Supplemental Information.

Immunofluorescence

C. jejuni 81-176 was TAMRA-labelled before a 3h infection of cells plated in Ibidi chamber μ -slides VI^{0.4} (Ibidi GmbH, Martinsried, Germany) in microaerophilic conditions. Samples were fixed with 2% formaldehyde for 30 min at 37°C. After washing, cells were permeabilized with 0.1% Triton X-100, blocked with 5% BSA and incubated for 3 h with primary antibodies. Mouse anti-p22^{phox}, affinity purified anti-Nox1 or anti-Duox1/2 rabbit antibodies were used for detection. Secondary antibody was Alexa Fluor 488-conjugated goat anti-rabbit IgG or Alexa Fluor 647-conjugated goat anti-mouse IgG (Invitrogen). Nuclei were stained with DAPI (Invitrogen). Further details are described in the online Supplemental Information.

Electron Microscopy

C. jejuni were fixed in ice-cold 2.5% glutaraldehyde, 1% paraformaldehyde in 0.1 M cacodylate buffer and left overnight at room temperature with gentle inversion. A freshly prepared saturated solution of Alcian Blue (Sigma-Aldrich) in de-ionized water was filtered through a 0.22 μ m pore size filter (Millipore) and was used as a positive stain for capsular polysaccharides. Samples were spread on carbon- and formvar-coated copper grids and washed with water. Samples were analyzed on a Tecnai12 Biotwin (FEI company) operating at 120 kV and images were acquired on a 4k \times 4k CCD Eagle camera (FEI company).

Statistical Analysis

Data are expressed as mean \pm SEM, n=3. Statistical differences between means were determined by a two-tailed Student's *t* test. Differences between multiple groups were tested using analysis of variance (ANOVA) for repeated measures. p values are indicated in figure legends.

Supplementary Material

Refer to Web version on PubMed Central for supplementary material.

Acknowledgments

We thank B. Wren, J.M. Bolla, P. Guerry, A. Stinzi, N. Dorrell, C. Szymanski, S. Backert, and D. Roos for kindly providing reagents, and S. Schuller, G. Rautureau and K. O'Neill for advice and technical assistance. The work was supported by Science Foundation Ireland (SFI PI Grant 04/IN3/B646) and the National Children Research Centre (both to B.B.), and an SFI Stokes award (to U.G.K.). T.H.S was funded by the EPSRC (Grant SB1738), J.M. was supported by Wellcome University Award. We would like to acknowledge staff and participating patients at the National Referral Center for Pediatric Gastroenterology, Our Lady's Children's Hospital Crumlin.

REFERENCES

- Al-Sayeqh AF, Loughlin MF, Dillon E, Mellits KH, Connerton IF. *Campylobacter jejuni* activates NF- κ B independently of TLR2, TLR4, Nod1 and Nod2 receptors. *Microb Pathog.* 2010; 49:294–304. [PubMed: 20599492]
- Bacon DJ, Szymanski CM, Burr DH, Silver RP, Alm RA, Guerry P. A phase-variable capsule is involved in virulence of *Campylobacter jejuni* 81-176. *Mol Microbiol.* 2001; 40:769–777. [PubMed: 11359581]
- Bae YS, Choi MK, Lee WJ. Dual oxidase in mucosal immunity and host-microbe homeostasis. *Trends Immunol.* 2010; 31:278–287. [PubMed: 20579935]
- Bechet E, Gruszczuk J, Terreux R, Gueguen-Chaignon V, Vigouroux A, Obadia B, Cozzone AJ, Nessler S, Grangeasse C. Identification of structural and molecular determinants of the tyrosine-kinase Wzc and implications in capsular polysaccharide export. *Mol Microbiol.* 2009a; 77:1315–1325. [PubMed: 20633230]
- Bechet E, Guiral S, Torres S, Mijakovic I, Cozzone AJ, Grangeasse C. Tyrosine-kinases in bacteria: from a matter of controversy to the status of key regulatory enzymes. *Amino Acids.* 2009b; 37:499–507. [PubMed: 19189200]
- Bedard K, Krause KH. The NOX family of ROS-generating NADPH oxidases: physiology and pathophysiology. *Physiol Rev.* 2007; 87:245–313. [PubMed: 17237347]
- Bernatchez S, Szymanski CM, Ishiyama N, Li J, Jarrell HC, Lau PC, Berghuis AM, Young NM, Wakarchuk WW. A single bifunctional UDP-GlcNAc/Glc 4-epimerase supports the synthesis of three cell surface glycoconjugates in *Campylobacter jejuni*. *J Biol Chem.* 2005; 280:4792–4802. [PubMed: 15509570]
- Bolla JM, De E, Dorez A, Pages JM. Purification, characterization and sequence analysis of Omp50, a new porin isolated from *Campylobacter jejuni*. *Biochem J.* 2000; 352(Pt 3):637–643. [PubMed: 11104668]
- Botteaux A, Hoste C, Dumont JE, Van Sande J, Allaoui A. Potential role of Noxes in the protection of mucosae: H₂O₂ as a bacterial repellent. *Microbes Infect.* 2009; 11:537–544. [PubMed: 19298864]
- Corcionivoschi N, Clyne M, Lyons A, Elmi A, Gundogdu O, Wren BW, Dorrell N, Karlyshev AV, Bourke B. *Campylobacter jejuni* cocultured with epithelial cells reduces surface capsular polysaccharide expression. *Infect Immun.* 2009; 77:1959–1967. [PubMed: 19273563]
- Cuthbertson L, Mainprize IL, Naismith JH, Whitfield C. Pivotal roles of the outer membrane polysaccharide export and polysaccharide copolymerase protein families in export of extracellular polysaccharides in gram-negative bacteria. *Microbiol Mol Biol Rev.* 2009; 73:155–177. [PubMed: 19258536]
- Fischer AJ, Lennemann NJ, Krishnamurthy S, Pocza P, Durairaj L, Launspach JL, Rhein BA, Wohlford-Lenane C, Lorentzen D, Banfi B, et al. Enhancement of Respiratory Mucosal Anti-viral Defenses by Iodide Oxidation. *Am J Respir Cell Mol Biol.* 2011; 45:874–881. [PubMed: 21441383]
- Flores MV, Crawford KC, Pullin LM, Hall CJ, Crosier KE, Crosier PS. Dual oxidase in the intestinal epithelium of zebrafish larvae has anti-bacterial properties. *Biochem Biophys Res Commun.* 2010; 400:164–168. [PubMed: 20709024]
- Galkin VE, Yu X, Bielnicki J, Heuser J, Ewing CP, Guerry P, Egelman EH. Divergence of quaternary structures among bacterial flagellar filaments. *Science.* 2008; 320:382–385. [PubMed: 18420936]
- Gianni D, Taulet N, DerMardirossian C, Bokoch GM. c-Src-mediated phosphorylation of NoxA1 and Tks4 induces the reactive oxygen species (ROS)-dependent formation of functional invadopodia in human colon cancer cells. *Mol Biol Cell.* 2010; 21:4287–4298. [PubMed: 20943948]
- Grangeasse C, Terreux R, Nessler S. Bacterial tyrosine-kinases: structure-function analysis and therapeutic potential. *Biochim Biophys Acta.* 2010; 1804:628–634. [PubMed: 19716442]
- Gruszczuk J, Fleurie A, Olivares-Illana V, Bechet E, Zanella-Cleon I, Morera S, Meyer P, Pompidor G, Kahn R, Grangeasse C, Nessler S. Structure analysis of the *Staphylococcus aureus* UDP-*N*-acetyl-mannosamine dehydrogenase Cap50 involved in capsular polysaccharide biosynthesis. *J Biol Chem.* 2011; 286:17112–17121. [PubMed: 21454499]

- Ha EM, Lee KA, Seo YY, Kim SH, Lim JH, Oh BH, Kim J, Lee WJ. Coordination of multiple dual oxidase-regulatory pathways in responses to commensal and infectious microbes in drosophila gut. *Nat Immunol.* 2009; 10:949–957. [PubMed: 19668222]
- Hooper LV, Macpherson AJ. Immune adaptations that maintain homeostasis with the intestinal microbiota. *Nat Rev Immunol.* 2010; 10:159–169. [PubMed: 20182457]
- Hu L, McDaniel JP, Kopecko DJ. Signal transduction events involved in human epithelial cell invasion by *Campylobacter jejuni* 81-176. *Microb Pathog.* 2006; 40:91–100. [PubMed: 16426812]
- Janssen R, Krogfelt KA, Cawthraw SA, van Pelt W, Wagenaar JA, Owen RJ. Host-pathogen interactions in *Campylobacter* infections: the host perspective. *Clin Microbiol Rev.* 2008; 21:505–518. [PubMed: 18625685]
- Keo T, Collins J, Kunwar P, Blaser MJ, Iovine NM. *Campylobacter* capsule and lipooligosaccharide confer resistance to serum and cationic antimicrobials. *Virulence.* 2011; 2:30–40. [PubMed: 21266840]
- Krause-Gruszczynska M, Rohde M, Hartig R, Genth H, Schmidt G, Keo T, Konig W, Miller WG, Konkel ME, Backert S. Role of the small Rho GTPases Rac1 and Cdc42 in host cell invasion of *Campylobacter jejuni*. *Cell Microbiol.* 2007; 9:2431–2444. [PubMed: 17521326]
- Lacour S, Bechet E, Cozzone AJ, Mijakovic I, Grangeasse C. Tyrosine phosphorylation of the UDP-glucose dehydrogenase of *Escherichia coli* is at the crossroads of colanic acid synthesis and polymyxin resistance. *PLoS ONE.* 2008; 3:e3053. [PubMed: 18725960]
- Lee DC, Jia Z. Emerging structural insights into bacterial tyrosine kinases. *Trends Biochem Sci.* 2009; 34:351–357. [PubMed: 19525115]
- Lee DC, Zheng J, She YM, Jia Z. Structure of *Escherichia coli* tyrosine kinase Etk reveals a novel activation mechanism. *EMBO J.* 2008; 27:1758–1766. [PubMed: 18497741]
- Lin MH, Hsu TL, Lin SY, Pan YJ, Jan JT, Wang JT, Khoo KH, Wu SH. Phosphoproteomics of *Klebsiella pneumoniae* NTUH-K2044 reveals a tight link between tyrosine phosphorylation and virulence. *Mol Cell Proteomics.* 2009; 8:2613–2623. [PubMed: 19696081]
- Marteyn B, Scorza FB, Sansonetti PJ, Tang C. Breathing life into pathogens: the influence of oxygen on bacterial virulence and host responses in the gastrointestinal tract. *Cell Microbiol.* 2011; 13:171–176. [PubMed: 21166974]
- Monteville MR, Yoon JE, Konkel ME. Maximal adherence and invasion of INT 407 cells by *Campylobacter jejuni* requires the CadF outer-membrane protein and microfilament reorganization. *Microbiology.* 2003; 149:153–165. [PubMed: 12576589]
- Nauseef WM. How human neutrophils kill and degrade microbes: an integrated view. *Immunol Rev.* 2007; 219:88–102. [PubMed: 17850484]
- Palyada K, Sun YQ, Flint A, Butcher J, Naikare H, Stintzi A. Characterization of the oxidative stress stimulon and PerR regulon of *Campylobacter jejuni*. *BMC Genomics.* 2009; 10:481. [PubMed: 19835633]
- Rada B, Leto TL. Oxidative innate immune defenses by Nox/Duox family NADPH oxidases. *Contrib Microbiol.* 2008; 15:164–187. [PubMed: 18511861]
- Rokutan K, Kawahara T, Kuwano Y, Tominaga K, Nishida K, Teshima-Kondo S. Nox enzymes and oxidative stress in the immunopathology of the gastrointestinal tract. *Semin Immunopathol.* 2008; 30:315–327. [PubMed: 18521607]
- Rosen H, Klebanoff SJ, Wang Y, Brot N, Heinecke JW, Fu X. Methionine oxidation contributes to bacterial killing by the myeloperoxidase system of neutrophils. *Proc Natl Acad Sci USA.* 2009; 106:18686–18691. [PubMed: 19833874]
- Rothfork JM, Timmins GS, Harris MN, Chen X, Lulis AJ, Otto M, Cheung AL, Gresham HD. Inactivation of a bacterial virulence pheromone by phagocyte-derived oxidants: new role for the NADPH oxidase in host defense. *Proc Natl Acad Sci USA.* 2004; 101:13867–13872. [PubMed: 15353593]
- Swanson PA 2nd, Kumar A, Samarin S, Vijay-Kumar M, Kundu K, Murthy N, Hansen J, Nusrat A, Neish AS. Enteric commensal bacteria potentiate epithelial restitution via reactive oxygen species-mediated inactivation of focal adhesion kinase phosphatases. *Proc Natl Acad Sci USA.* 2011; 108:8803–8808. [PubMed: 21555563]

- Tolkatchev D, Shaykhtudinov R, Xu P, Plamondon J, Watson DC, Young NM, Ni F. Three-dimensional structure and ligand interactions of the low molecular weight protein tyrosine phosphatase from *Campylobacter jejuni*. *Protein Sci.* 2006; 15:2381–2394. [PubMed: 17008719]
- Ueyama T, Geiszt M, Leto TL. Involvement of Rac1 in activation of multicomponent Nox1- and Nox3-based NADPH oxidases. *Mol Cell Biol.* 2006; 26:2160–2174. [PubMed: 16507994]
- Voisin S, Watson DC, Tessier L, Ding W, Foote S, Bhatia S, Kelly JF, Young NM. The cytoplasmic phosphoproteome of the Gram-negative bacterium *Campylobacter jejuni*: evidence for modification by unidentified protein kinases. *Proteomics.* 2007; 7:4338–4348. [PubMed: 17973292]
- von Lohneysen K, Noack D, Wood MR, Friedman JS, Knaus UG. Structural insights into Nox4 and Nox2: motifs involved in function and cellular localization. *Mol Cell Biol.* 2010; 30:961–975. [PubMed: 19995913]
- Watson RO, Galan JE. *Campylobacter jejuni* survives within epithelial cells by avoiding delivery to lysosomes. *PLoS Pathog.* 2008; 4:e14. [PubMed: 18225954]
- Winter SE, Thiennimitr P, Winter MG, Butler BP, Huseby DL, Crawford RW, Russell JM, Bevins CL, Adams LG, Tsolis RM, et al. Gut inflammation provides a respiratory electron acceptor for *Salmonella*. *Nature.* 2010; 467:426–429. [PubMed: 20864996]
- Xu Y, Szep S, Lu Z. The antioxidant role of thiocyanate in the pathogenesis of cystic fibrosis and other inflammation-related diseases. *Proc Natl Acad Sci USA.* 2009; 106:20515–20519. [PubMed: 19918082]
- Young KT, Davis LM, Dirita VJ. *Campylobacter jejuni*: molecular biology and pathogenesis. *Nat Rev Microbiol.* 2007; 5:665–679. [PubMed: 17703225]

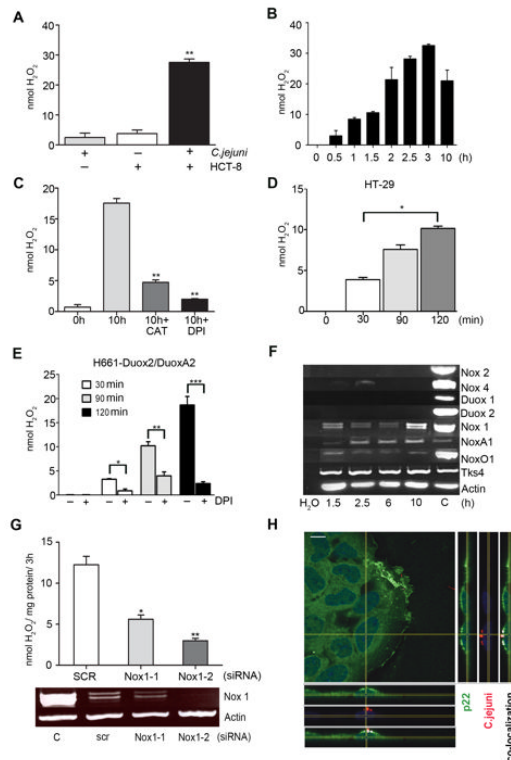


Figure 1. Exposure of intestinal cells to *C. jejuni* 81-176 leads to NADPH oxidase-mediated release of hydrogen peroxide

(A) H_2O_2 production after co-culture of *C. jejuni* with HCT-8 cells for 10 h. Statistical significance relative to non-inhibited H_2O_2 production is indicated, $**P<0.0001$, $n=3$, \pm S.E.M. (B) Time course of H_2O_2 release from HCT-8 cells during co-culture with *C. jejuni*. (C) H_2O_2 production after co-culture of *C. jejuni* with HCT-8 cells for 10 h in the presence of inhibitors. Catalase (CAT) and DPI were added prior to exposure to bacteria, $**P<0.0001$, $n=3$, \pm S.E.M. (D) H_2O_2 release from HT-29 cells during co-culture with *C. jejuni* at various time points, $*P=0.0005$, $n=3$, \pm S.E.M. (E) H_2O_2 release from H661-Duox2/DuoxA2 cells during co-culture with *C. jejuni* at various time points, $*P=0.0005$, $**P=0.0001$, $***P=0.00005$, $n=3$, \pm S.E.M. Preincubation with DPI ($15\ \mu\text{M}$, 30 min) was used as control. (F) Semi-quantitative RT-PCR for expression of Nox/Duox and functionally associated genes in HCT-8 cells. Actin served as loading control and cDNA (C) or plasmid cDNA was used as gene-specific PCR control. (G) Knockdown of Nox1 in HCT-8 cells using Nox1-1, Nox1-2 and scrambled siRNA followed by H_2O_2 measurement. Actin PCR and independent control PCR (C) are shown. Statistical significance is relative to SCR siRNA. $*P=0.0005$ and $**P=0.0001$, $n=3$, \pm S.E.M. (H) Confocal analysis of the Nox1-p22^{phox} complex and TAMRA-labeled *C. jejuni* (red) in HCT-8 cells after 3 h of exposure (co-localization in white). Anti-p22^{phox} staining (green), nuclei (DAPI, blue), scale bar $10\ \mu\text{m}$. See also Figure S1.

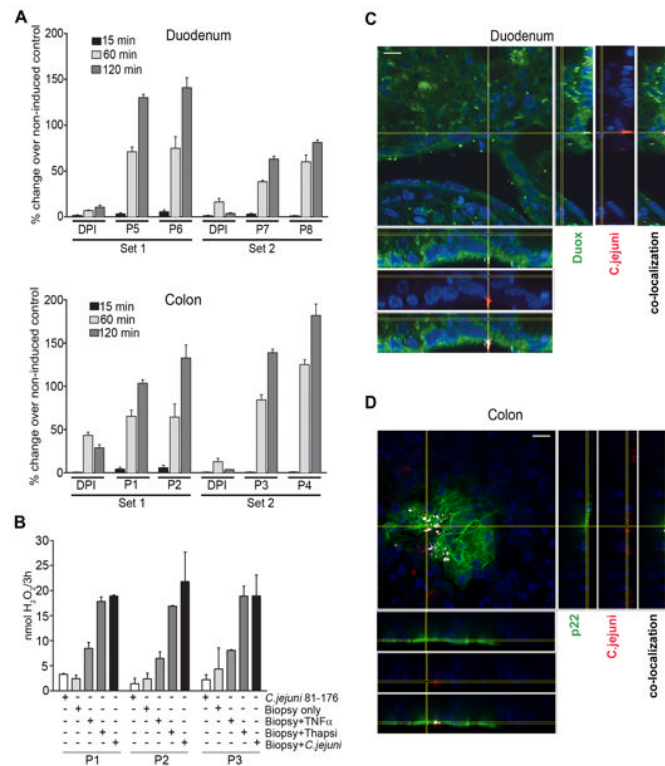


Figure 2. Release of NADPH oxidase-mediated hydrogen peroxide in an *ex vivo* model of gastrointestinal epithelium after exposure to *C. jejuni*

(A) H_2O_2 generation in colonic and duodenal biopsies mounted as pIVOC and incubated with *C. jejuni*. The percentage change of H_2O_2 over time with or without DPI is shown. Non-infected control biopsies were taken as base line. Data are representative of four sets from eight patients (P 1-8), error bars represent \pm S.D. of 3 independent measurements per time point. (B) H_2O_2 release from duodenum biopsies of 3 different patients (P) either without stimulation, stimulated with TNF α (40 ng/ml), thapsigargin (25 μ M), or co-cultured with *C. jejuni* for 3 h. Error bars represent \pm S.D. of 3 independent measurements per treatment. (C) Immunofluorescence of duodenal pIVOC biopsy infected with *C. jejuni* for 3 h and stained for Duox2 (green) and *C. jejuni* (red). Scale bar 10 μ m. (D) Immunofluorescence of colonic pIVOC biopsy infected with *C. jejuni* for 3 h and stained for p22^{phox} (green) and *C. jejuni* (red). Co-localization is indicated in white, scale bar 10 μ m. See also Figure S2.

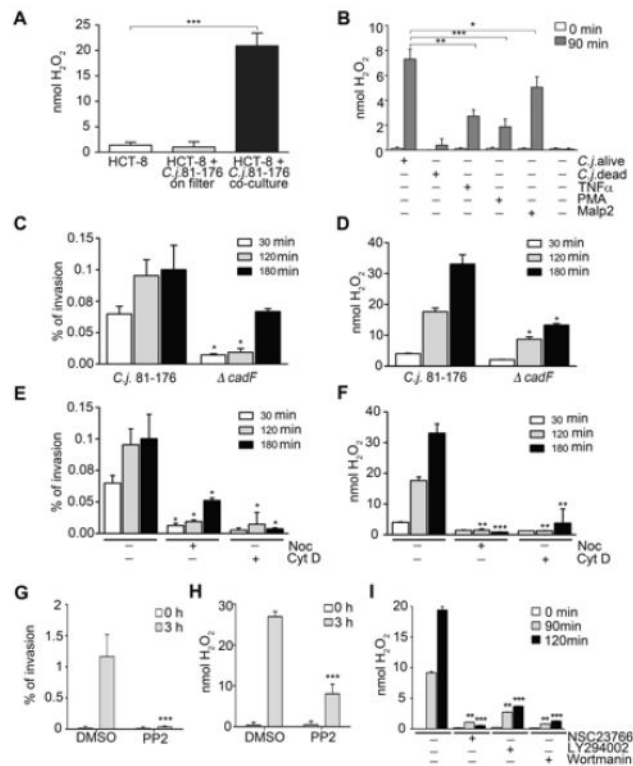


Figure 3. Active contact of *C. jejuni* 81-176 with HCT-8 cells is required for H₂O₂ production (A) H₂O₂ release by HCT-8 cells in the absence of *C. jejuni*, in the presence of *C. jejuni* separated from cells using a 0.2 μ m filter, or when *C. jejuni* is co-cultured in contact with cells, ** $P < 0.0001$, $n = 3$, \pm S.E.M. (B) H₂O₂ release by HCT-8 cells stimulated with TNF α (40 ng/ml), PMA (0.1 ng/ml), Malp2 (10 ng/ml), live *C. jejuni* or heat-killed *C. jejuni* (MOI 100). One-way ANOVA ($P < 0.0001$) and a two-tailed non-parametric t test were used, $n = 3$, * $P = 0.005$, ** $P = 0.0001$, *** $P = 0.00005$. (C-I) Invasion of *C. jejuni* correlates with H₂O₂ release. Invasion is expressed as % of inoculum. (C, D) Comparison of wildtype *C. jejuni* with invasion-deficient *C. jejuni* $\Delta cadF$ in HCT-8 cells. (E – I) Pretreatment of HCT-8 cells with indicated inhibitors (nocodazole, cytochalasin D, PP2, NSC23766, LY294002, wortmannin) for 45 min followed by incubation with *C. jejuni*, Two-tailed non-parametric t test in C-I, *** $P < 0.0001$, ** $0.001 < P < 0.0001$, * $0.005 < P < 0.001$ $n = 3$, \pm S.E.M. When not otherwise specified, the non treated sample was compared to the treated sample. See also Figure S3.

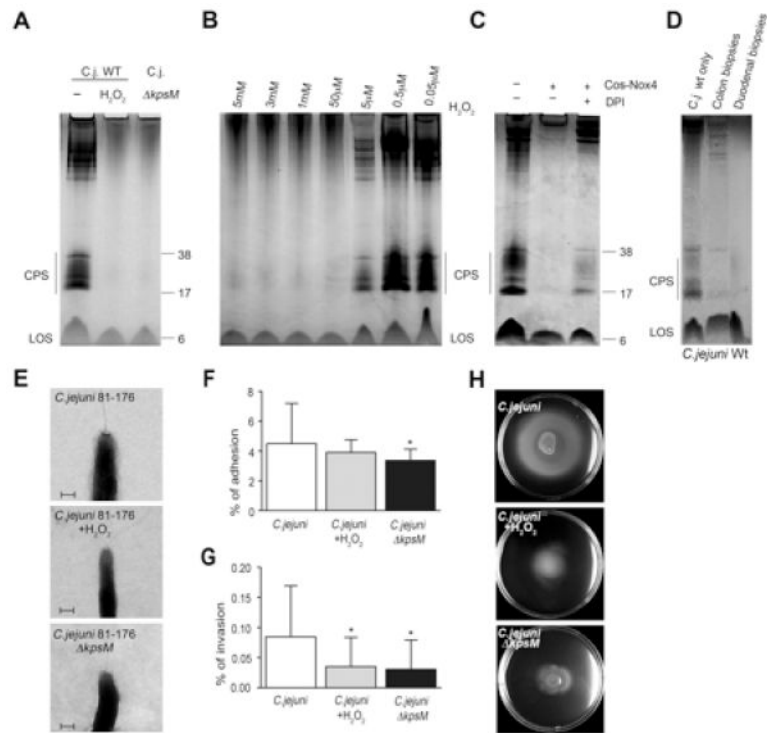


Figure 4. Exposure of *C. jejuni* 81-176 to H_2O_2 leads to loss of bacterial capsule and decreased motility and invasion

(A) Capsule polysaccharide (CPS) staining using lysates derived from *C. jejuni* with or without exposure to 5 mM H_2O_2 (10 h). For comparison capsule-deficient *C. jejuni* $\Delta kpsM$ was used. Lipooligosaccharide (LOS) is indicated. (B) H_2O_2 concentration-dependent loss of CPS staining in *C. jejuni* lysates (10h exposure). (C) *C. jejuni* was exposed to H_2O_2 released from constitutively active Nox4 (Cos-Nox4 cells), followed by CPS staining. Cells and bacteria were physically separated using a 0.3 μm filter. DPI preincubation of Cos-Nox4 cells for 30 min and inhibitor wash-out was used as control. (D) CPS staining of lysates derived from extracellular *C. jejuni* after exposure to colon or duodenal biopsies (8h). (E) Electron microscopy images of *C. jejuni* with and without exposure to 5 mM H_2O_2 . *C. jejuni* $\Delta kpsM$ was used for comparison. Scale bar 200 nm. (F-H) Adhesion, invasion and motility of *C. jejuni*, H_2O_2 -exposed *C. jejuni* and *C. jejuni* $\Delta kpsM$ in HCT-8 cells. Adhesion and invasion are expressed as % of inoculum. * $P=0.01$, $n=3$, \pm S.E.M. See also Figure S4.

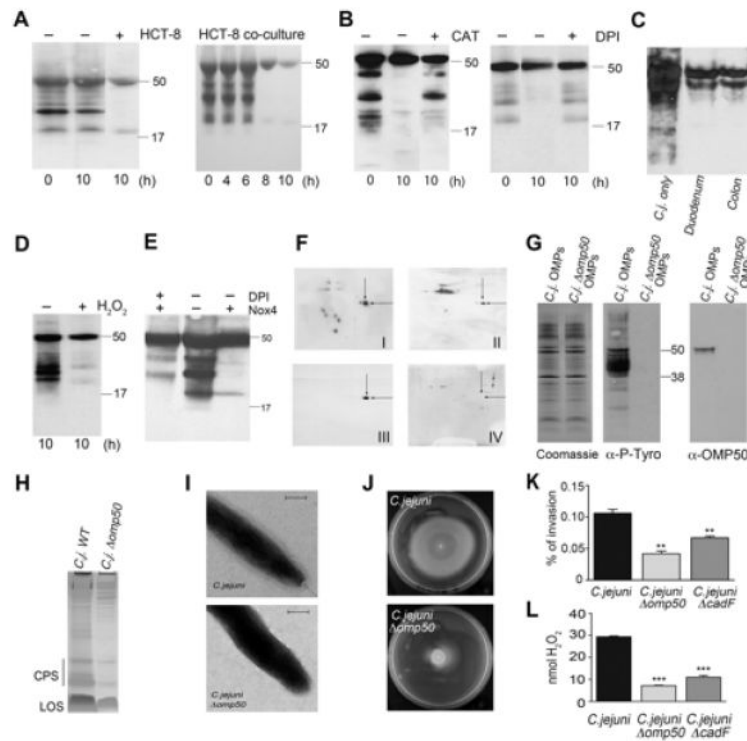


Figure 5. ROS-mediated disruption of phosphotyrosine signaling by Cj1170 (OMP50), a bacterial tyrosine kinase controlling capsule synthesis
 (A – E) Exposure of *C. jejuni* to H_2O_2 alters bacterial tyrosine phosphorylation. (A) Time course of co-culture of *C. jejuni* with HCT-8 cells. Tyrosine phosphorylation of outer membrane proteins (OMPs) is shown. (B) Phosphotyrosine incorporation in *C. jejuni* OMPs derived from HCT-8 co-cultures in the absence or presence of catalase or DPI pretreatment. (C) Phosphotyrosine content of *C. jejuni* exposed to medium (*C. j.* only) or of extracellular *C. jejuni* collected after 6h of infection of duodenal or colon biopsies. (D-E) Exposure of *C. jejuni* to 5 mM H_2O_2 (D) or to Cos-Nox4 cells separated by a filter (E) for 10 h followed by OMP extraction and phosphotyrosine detection with or without DPI pretreatment. (F) Phosphotyrosine 2D immunoblots of *C. jejuni* OMPs without treatment (I) and after co-culture with HCT-8 cells (II). Blot (I) was stripped and re-probed with OMP50 antibody (III). The indicated spot was also analyzed by MS-MS. *C. jejuni* $\Delta omp50$ OMPs were run on 2D gels and blotted with OMP50 antibody (IV). (G) Coomassie, anti-phosphotyrosine and anti-OMP50 immunoblots of OMPs derived from *C. jejuni* wt and *C. jejuni* $\Delta omp50$. (H) CPS staining of *C. jejuni* and *C. jejuni* $\Delta omp50$ lysates. (I) Electron microscopy images of *C. jejuni* and *C. jejuni* $\Delta omp50$. Scale bar 200 nm. (J, K) Comparison of wildtype *C. jejuni* with *C. jejuni* $\Delta omp50$ regarding motility in soft agar and HCT-8 invasion. (L) ROS generation after co-culture of indicated *C. jejuni* strains with HCT-8 cells. Adhesion- and invasion-deficient *C. jejuni* $\Delta cadF$ served as control. Invasion is expressed as % of inoculum. ** $P=0.0003$, *** $P<0.0001$ $n=3$, \pm S.E.M. See also Figure S5.

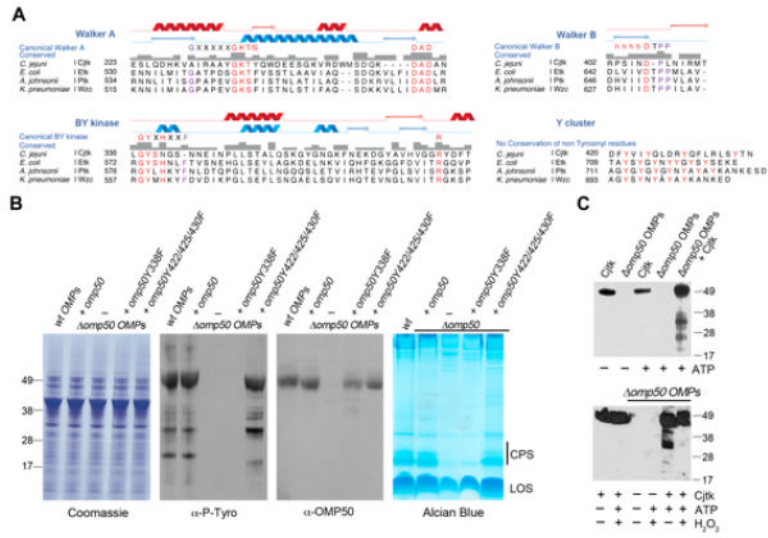


Figure 6. Cjtk (OMP50) represents a unique outer membrane BY-kinase
 (A) Alignment of typical BY-kinase motifs in *E.coli* Etk, *A. johnsonii* Ptk, *K. pneumoniae* Wzc with *C. jejuni* OMP50 (Cjtk). Etk secondary structure is in blue and prediction for Cjtk in red (see also Figure S6). (B) Identification of the active site tyrosine in Cjtk. *C. jejuni* $\Delta omp50$ strain was complemented with *omp50* wildtype or indicated *omp50* mutants, followed by Coomassie blue staining, anti-phosphotyrosine and anti-OMP50 immunoblotting of OMP fractions, and by Alcian blue staining of capsular polysaccharides. (C) OMP phosphorylation by purified Cjtk is redox-sensitive. *In vitro* phosphorylation of *C. jejuni* $\Delta omp50$ OMPs by purified Cjtk (anti-phosphotyrosine blot) in the presence (bottom panel) or absence (top panel) of 10 mM H₂O₂. See also Figure S6.

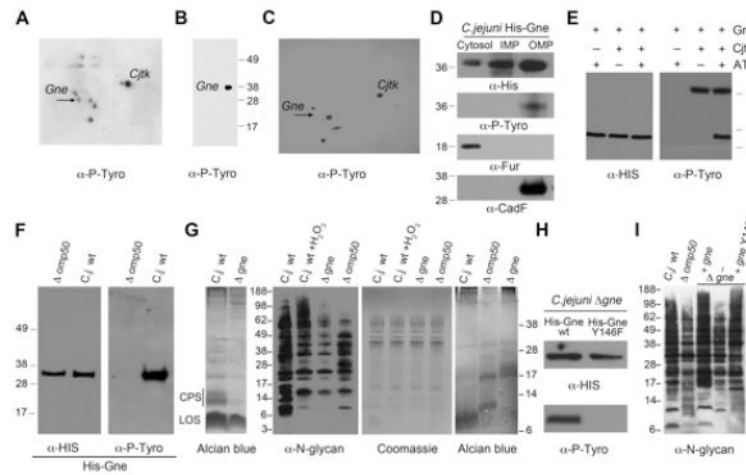


Figure 7. Activity of UDP-GlcNAc/Glc 4-epimerase (Gne) is positively regulated by Cjtk-mediated phosphorylation of the active site tyrosine 146

(A, B) Phosphotyrosine detection after 2D separation of *C. jejuni* OMP lysates. Arrow indicates spot recovered for MS-MS analysis and identified as Cj1131c (Gne). The extracted spot was run in 1D SDS-PAGE and blotted with anti-phosphotyrosine antibody (B). (C) 2D separation and phosphotyrosine detection of OMPs derived from deletion mutant *C. jejuni* $\Delta galE/gne$. Arrow indicates the missing spot corresponding to Gne protein. (D) Cytoplasm, IMP and OMP preparations of *C. jejuni* expressing histidine-tagged Gne were probed with anti-His and anti-phosphotyrosine antibodies. An anti-Fur and anti-CadF antibodies were used as control to assess the purity of the fractions. (E) Purified Cjtk and *E. coli* purified His-Gne were subjected to *in vitro* kinase assays and probed with anti-phosphotyrosine and anti-His antibody. (F) OMPs were prepared from wildtype *C. jejuni* and *C. jejuni* $\Delta omp50$, both expressing histidine-tagged Gne. His-Gne was affinity purified and visualized with anti-phosphotyrosine and anti-His antibody (see also Figure S7). (G) Comparative analysis of carbohydrate structures in *C. jejuni* wildtype, *C. jejuni* wt exposed to H_2O_2 , and *C. jejuni* mutants $\Delta omp50$ and Δgne . Left panel: Alcian blue gel of CPS profile; middle panels: N-glycosylation blot profile and corresponding Coomassie gel; right panel: Alcian blue gel of LOS profile. (H) *In vivo* phosphorylation of Gne was assessed by immunoblotting using *C. jejuni* Δgne reconstituted with either His-Gne wt or His-Gne Y146F and subsequent affinity purification of wt or mutant His-Gne. (I) N-glycosylation profile of *C. jejuni* wt or $\Delta omp50$, compared to *C. jejuni* Δgne and to Δgne reconstituted with His-Gne wt or with His-Gne Y146F. Arrows indicate variations of glycosylation on $\Delta omp50$ and Δgne Y146F when compared to the wt and Gne reconstituted *C. jejuni*. See also Figure S7.